



# In situ luminescence measurement of irradiation defects in ternary lithium ceramics under ion beam irradiation

Kimikazu Moritani <sup>a</sup>, Hirotake Moriyama <sup>b,\*</sup>

<sup>a</sup> Faculty of Engineering, Kyoto University, Yoshida, Sakyo-ku, Kyoto 606-01, Japan

<sup>b</sup> Research Reactor Institute, Kyoto University, Kumatori-cho, Sennan-gun, Osaka 590-04, Japan

## Abstract

For the performance assessment of fusion reactor solid breeder materials, the production behavior of irradiation defects in some candidate materials of  $\text{Li}_2\text{TiO}_3$ ,  $\text{Li}_2\text{ZrO}_3$  and  $\text{Li}_2\text{SnO}_3$  was studied by an in situ luminescence measurement technique under ion beam irradiation. The luminescence was observed to be composed of multiple luminescence bands and the temperature dependence of the luminescence intensity was measured under  $\text{He}^+$  or  $\text{H}^+$  ion beam irradiation. The production mechanism of irradiation defects was discussed by comparing the present results with those previously obtained for  $\text{Li}_2\text{O}$ . The effects of irradiation defects on tritium recovery kinetics and material stability were pointed out. © 1997 Elsevier Science B.V.

## 1. Introduction

In a fusion reactor solid blanket system, tritium breeding lithium ceramics are attacked by high energy neutrons and energetic particles from nuclear reactions and severe irradiation damage may be expected. The irradiation behavior of lithium ceramics is thus important for the performance assessment of fusion reactor blanket systems. The effects of irradiation on the tritium release behaviors and microstructural changes of lithium ceramics are particularly important.

For a clearer understanding of such effects, we have studied the production behavior of irradiation defects in  $\text{Li}_2\text{O}$  [1,2],  $\text{LiAlO}_2$  [3],  $\text{Li}_2\text{SiO}_3$  and  $\text{Li}_4\text{SiO}_4$  [4,5] by an in situ luminescence measurement technique under ion beam irradiation. In  $\text{Li}_2\text{O}$  and  $\text{LiAlO}_2$ , it has been confirmed that the  $\text{F}^+$  center (an oxygen vacancy trapping an electron) and the  $\text{F}^0$  center (an oxygen vacancy trapping two electrons), which are commonly observed in ionic crystals, are formed by irradiation. Similarly, the irradiation

defects of the  $\text{E}'$  center ( $\equiv\text{Si}\cdot$ ), the non-bridging oxygen hole center ( $\equiv\text{Si}-\text{O}\cdot$ ) and the peroxy radical ( $\equiv\text{Si}-\text{O}-\text{O}\cdot$ ) are produced in  $\text{Li}_2\text{SiO}_3$  and  $\text{Li}_4\text{SiO}_4$ . These defects are considered to play an important role in the tritium behavior. For comparison, the production behavior of irradiation defects in the lithium ceramics of  $\text{Li}_2\text{TiO}_3$ ,  $\text{Li}_2\text{ZrO}_3$  and  $\text{Li}_2\text{SnO}_3$  has been studied in the present study.

## 2. Experimental

The lithium ceramics of  $\text{Li}_2\text{TiO}_3$ ,  $\text{Li}_2\text{ZrO}_3$  and  $\text{Li}_2\text{SnO}_3$  were prepared by solid-state reactions. Powders of  $\text{TiO}_2$ ,  $\text{ZrO}_2$  or  $\text{SnO}_2$  of reagent grade obtained from Nacalai Tesque were milled with  $\text{Li}_2\text{CO}_3$  in stoichiometric amounts and calcined at 1123 K (950°C) for 8 h. The formation of each compound was confirmed by X-ray diffraction. Pellet-type samples of 10 mm in diameter and about 1 mm in thickness were sintered at 1423 K (1150°C) for 8 h. A  $\text{He}^+$  or  $\text{H}^+$  ion beam, accelerated with a Van de Graaff accelerator, was led to the target sample at 90°. The size of the ion beam was about 3 mm in diameter and the beam current was monitored. The luminescence from the target sample was led to monochromators, Ritsu MC-20N

\* Corresponding author. Fax: +81-724 51 2424.

and counted with photo-multipliers, Hamamatsu R585. The temperature of the sample holder was controlled with an electric heater and a thermocouple and another thermocouple was attached to the sample surface to monitor its temperature.

### 3. Results

#### 3.1. Analysis of luminescence bands

Figs. 1–3 show a set of typical luminescence spectra of  $\text{Li}_2\text{TiO}_3$ ,  $\text{Li}_2\text{ZrO}_3$  and  $\text{Li}_2\text{SnO}_3$  under  $\text{H}^+$  and  $\text{He}^+$  ion

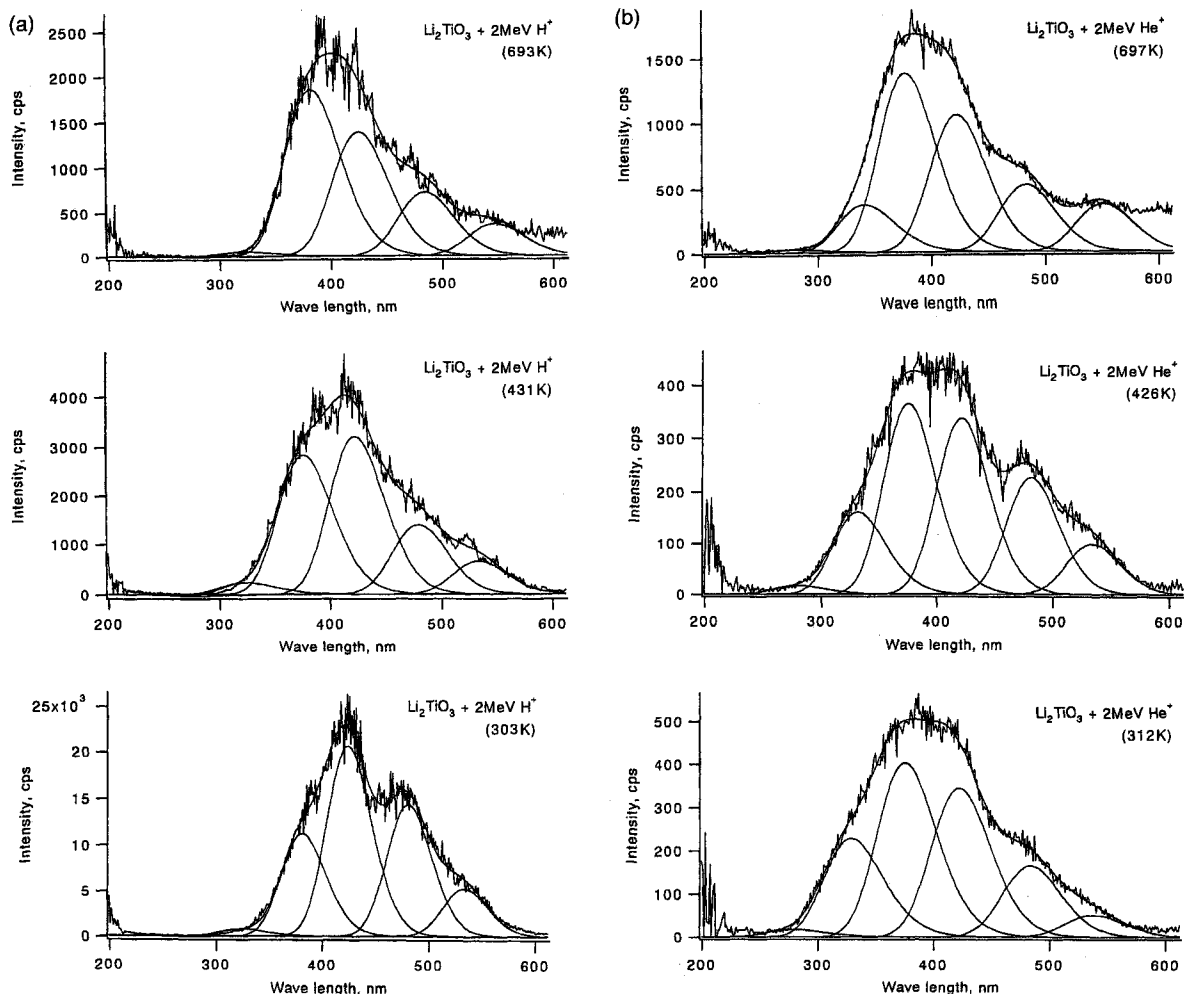


Fig. 1. Luminescence spectra of  $\text{Li}_2\text{TiO}_3$  under (a)  $\text{H}^+$  and (b)  $\text{He}^+$  irradiation.

Table 1  
Comparison of luminescence bands

Ceramics	Projectile ions	Luminescence bands (nm)						Note
$\text{Li}_2\text{O}$	$\text{He}^+$	(260)	340	380			(510)	Refs. [1,2]
$\text{Li}_2\text{SiO}_3$	$\text{H}^+$			380	420	490		Ref. [5]
	$\text{He}^+$		330	380	430	490		Ref. [4]
$\text{Li}_2\text{TiO}_3$	$\text{H}^+$	(280)	(325)	$378 \pm 4$	$423 \pm 3$	$482 \pm 4$	$536 \pm 4$	present
	$\text{He}^+$	(280)	$335 \pm 7$	$376 \pm 3$	$421 \pm 2$	$481 \pm 2$	$535 \pm 3$	present
$\text{Li}_2\text{ZrO}_3$	$\text{H}^+$	(280)	$327 \pm 4$	$371 \pm 5$	$421 \pm 3$	$483 \pm 8$	$541 \pm 6$	present
	$\text{He}^+$	$276 \pm 6$	$319 \pm 5$	$366 \pm 5$	$416 \pm 3$	$478 \pm 3$	$531 \pm 2$	present
$\text{Li}_2\text{SnO}_3$	$\text{H}^+$	(280)	(320)	$376 \pm 3$	$421 \pm 4$	$477 \pm 5$	$536 \pm 7$	present
	$\text{He}^+$	$278 \pm 7$	$321 \pm 4$	$371 \pm 4$	$421 \pm 2$	$485 \pm 4$	$540 \pm 5$	present

beam irradiation. The ordinate represents luminescence intensity corrected for beam current. The peak heights have been observed to be proportional to the beam current and then all of the spectra in the present study are corrected with the beam current for comparison.

The luminescence spectra are composed of multiple luminescence bands, as shown in Figs. 1–3. The decomposition of the spectra has been performed by least-squares fittings. Energy-based Gaussian functions were taken for all the luminescence bands and the peak heights and positions were determined. For a proper convergence, the peak width has been assumed to be given by an empirical correlation that  $y = cx^{-2}$  where  $y$  denotes the peak width in eV,  $x$  the peak position in eV and  $c$  the constant. The observed luminescence bands are summarized in Table 1 together with those of  $\text{Li}_2\text{O}$  [1] and  $\text{Li}_2\text{SiO}_3$  [4,5].

### 3.2. Temperature dependence of luminescence intensity

Figs. 4–6 show the Arrhenius plots of the luminescence intensity for  $\text{Li}_2\text{TiO}_3$ ,  $\text{Li}_2\text{ZrO}_3$  and  $\text{Li}_2\text{SnO}_3$  under  $\text{H}^+$  and  $\text{He}^+$  ion beam irradiation. The luminescence intensity corresponds to the peak height determined above. By comparing Figs. 4–6, the observed temperature dependent behaviors are summarized as follows.

(1) The temperature dependence of luminescence intensity under  $\text{He}^+$  ion irradiation is different from that under  $\text{H}^+$  ion irradiation; the luminescence intensity under  $\text{He}^+$  ion irradiation rises at temperatures around 700 K while it decreases rather monotonically with increasing temperature under  $\text{H}^+$  irradiation.

(2) In the temperature range where the luminescence intensity increases under  $\text{He}^+$  irradiation, luminescence

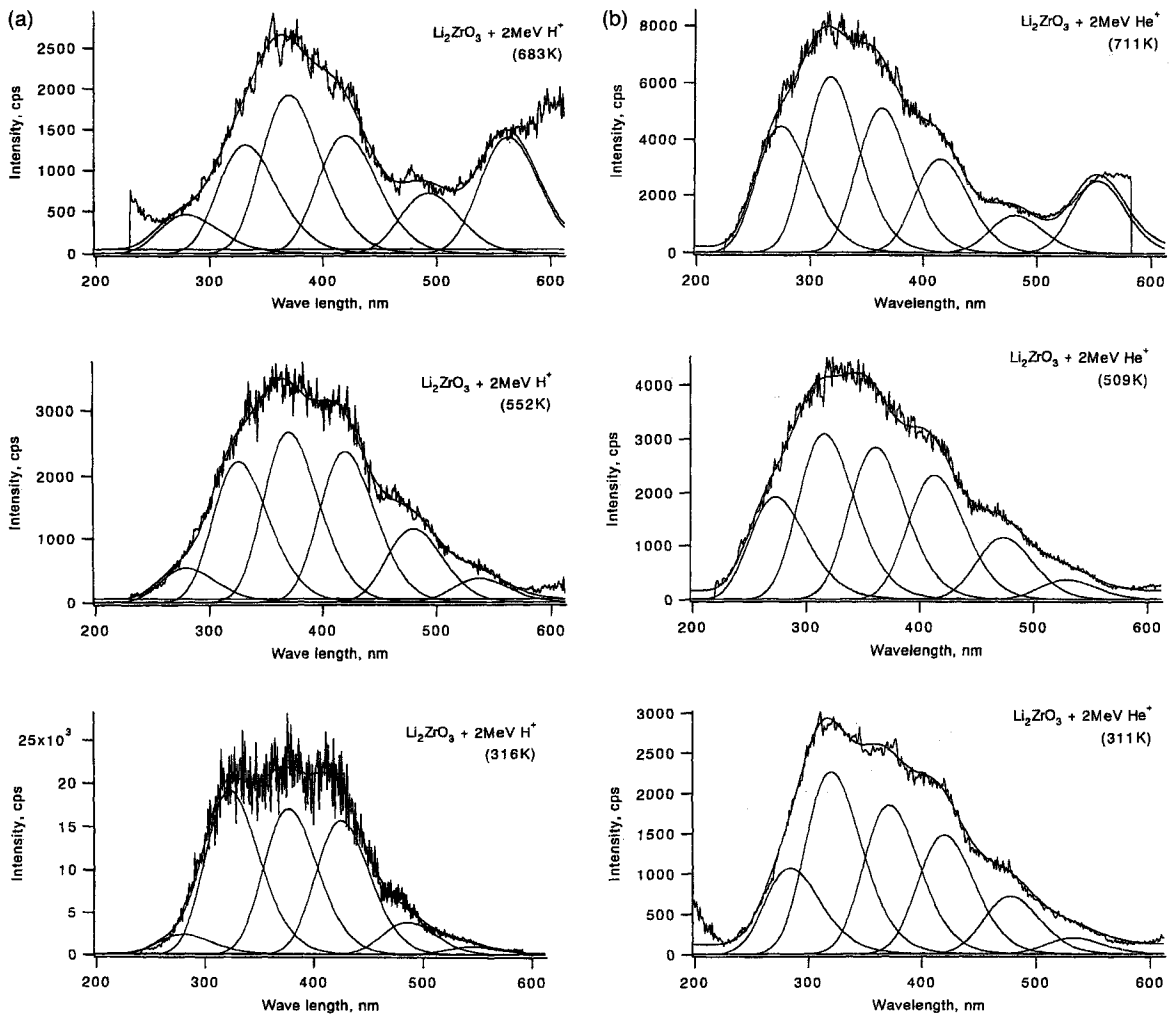


Fig. 2. Luminescence spectra of  $\text{Li}_2\text{ZrO}_3$  under (a)  $\text{H}^+$  and (b)  $\text{He}^+$  irradiation.

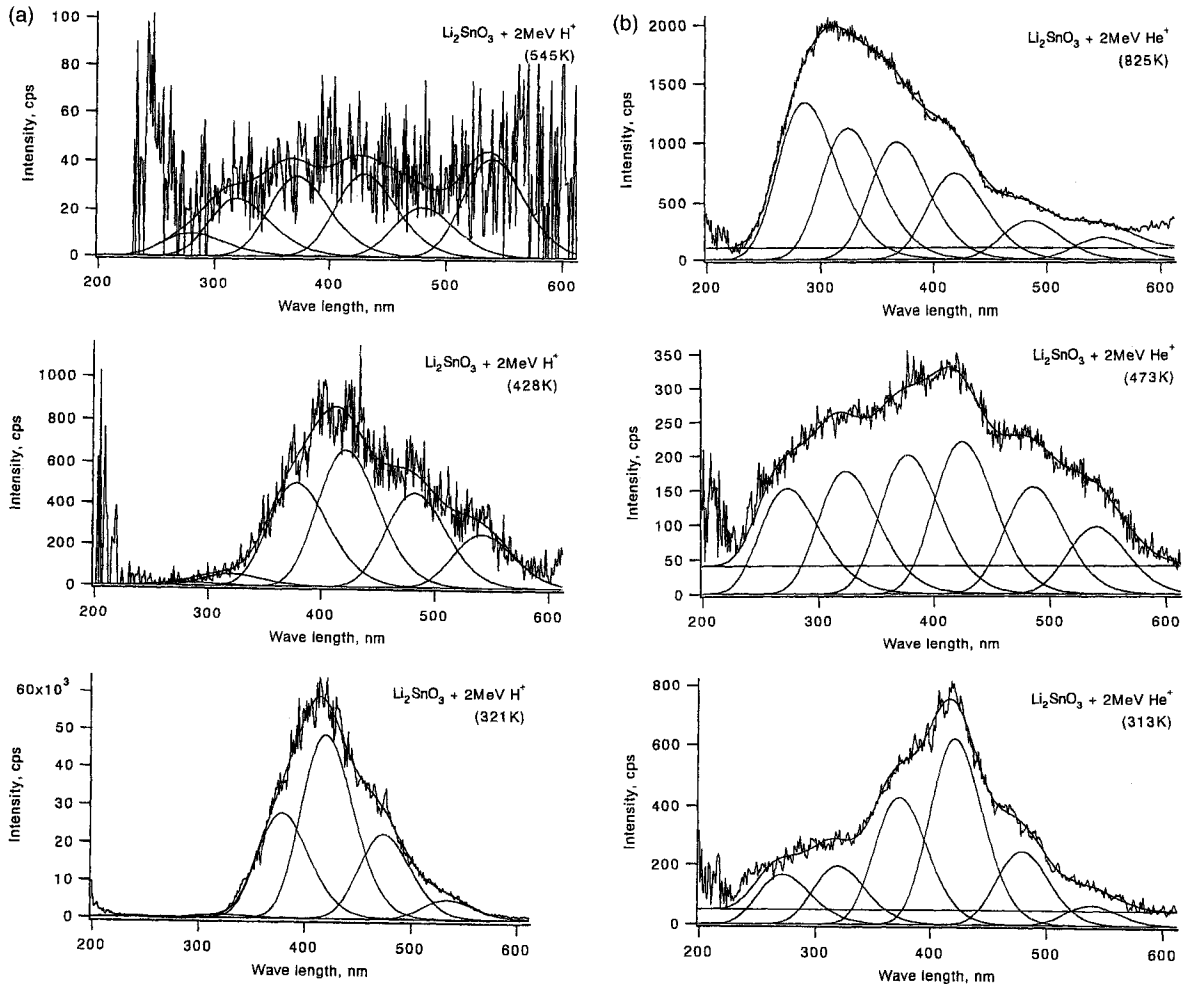


Fig. 3. Luminescence spectra of  $\text{Li}_2\text{SnO}_3$  under (a)  $\text{H}^+$  and (b)  $\text{He}^+$  irradiation.

bands of shorter wave length (shorter than 340 nm) are observed in the spectra.

(3) Under  $\text{H}^+$  irradiation, the temperature dependence of the luminescence intensity is different among the materials; the luminescence intensity decreases more rapidly in  $\text{Li}_2\text{SnO}_3$  with increasing temperature than in the other two.

## 4. Discussion

### 4.1. Luminescence bands and irradiation defects

The luminescence spectra have been decomposed successfully and it is important to address the observed luminescence bands to defect species. Various types of defect species may be considered in the present materials. In the case of  $\text{Li}_2\text{O}$  [1,2] and  $\text{LiAlO}_2$  [3], for example, the formation of F-type centers, i.e.,  $\text{F}^+$  centers and  $\text{F}^0$  cen-

ters, has been reported in the temperature range up to the blanket operating temperatures. In addition to these, the formation of self-trapped excitons has also been reported below the room temperature [6]. In  $\text{Li}_2\text{SiO}_3$  and  $\text{Li}_4\text{SiO}_4$  [4,5], furthermore, the formation of  $\text{E}'$  centers, non-bridging oxygen hole centers and peroxy radicals is considered and it has been suggested that the luminescence is associated with the formation of peroxy species in these materials in the temperature range from 300 to 850 K. Thus, various types of defect species are considered to be formed in  $\text{Li}_2\text{TiO}_3$ ,  $\text{Li}_2\text{ZrO}_3$  and  $\text{Li}_2\text{SnO}_3$  and it still remains unclear to which defect species the luminescence bands are addressed.

Although the luminescence spectra have been decomposed to a number of the luminescence bands, some of these seem to exhibit similar temperature dependences with one another in each material, as shown in Figs. 4–6. Consequently, rather similar origins may be suggested for these luminescence bands. This may be explained by con-

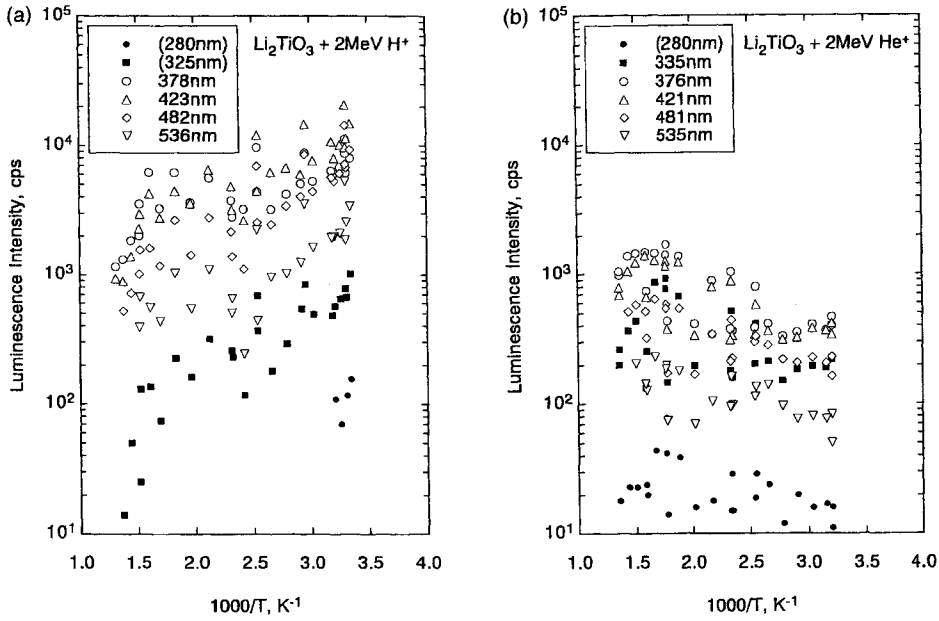


Fig. 4. Arrhenius plots of luminescence intensity of  $\text{Li}_2\text{TiO}_3$  under (a)  $\text{H}^+$  and (b)  $\text{He}^+$  irradiation.

sidering the microscopic structures of the materials. The structural arrangement of  $\text{Li}_2\text{TiO}_3$ ,  $\text{Li}_2\text{ZrO}_3$  and  $\text{Li}_2\text{SnO}_3$  is NaCl-like. In these compounds, the oxygen atoms form a distorted cubic close-packed network and the cations occupy, in an ordered fashion, all octahedral sites present

in this network [7,8]. The distorted network and the different distribution of the lithium and the tetravalent cations in the network will be the reason for the different luminescence bands of similar origins. In  $\text{Li}_2\text{TiO}_3$ , for example, the octahedral edges are shared between two Ti ions, two

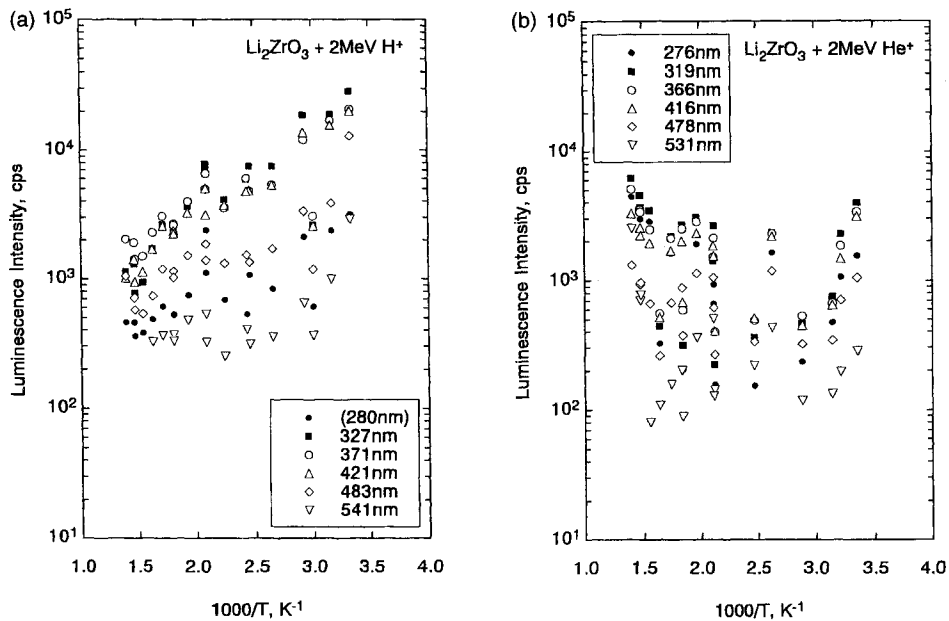


Fig. 5. Arrhenius plots of luminescence intensity of  $\text{Li}_2\text{ZrO}_3$  under (a)  $\text{H}^+$  and (b)  $\text{He}^+$  irradiation.

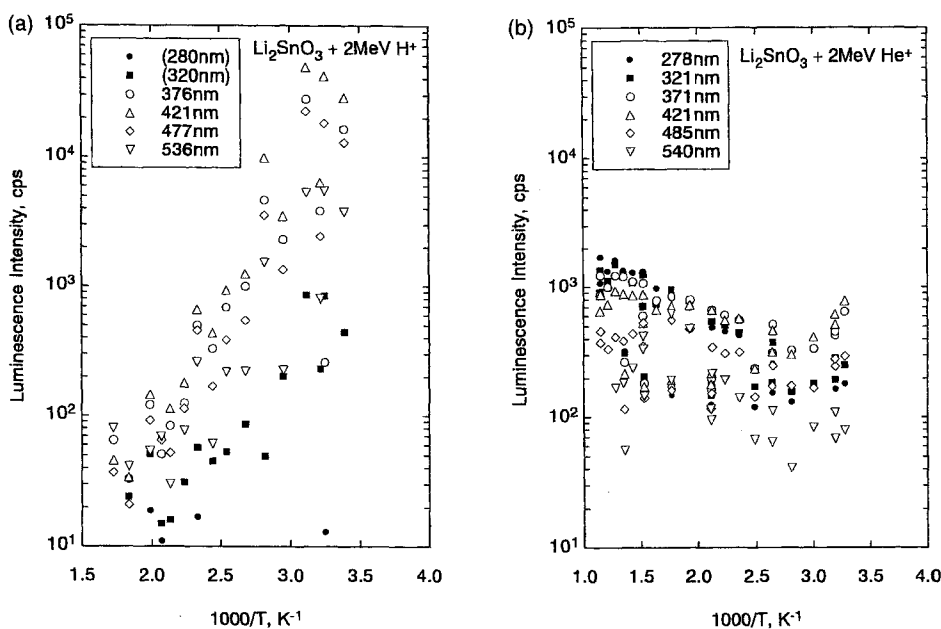
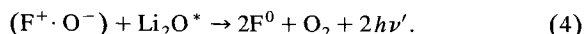
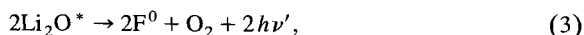
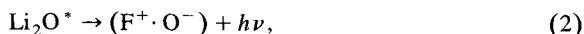


Fig. 6. Arrhenius plots of luminescence intensity of  $\text{Li}_2\text{SnO}_3$  under (a)  $\text{H}^+$  and (b)  $\text{He}^+$  irradiation.

Li ions, or one Ti and one Li ions and the mean O–O distances for the three categories are 2.58, 3.11 and 2.82 Å, respectively [8]. These differences will result in the observed variety of the luminescence bands. In addition to these, the structural rearrangement may also be taken into account under irradiation.

#### 4.2. Production mechanism of irradiation defects

The production mechanisms of irradiation defects in  $\text{Li}_2\text{O}$  [1,2],  $\text{LiAlO}_2$  [3],  $\text{Li}_2\text{SiO}_3$  and  $\text{Li}_4\text{SiO}_4$  [4,5] have been studied in our previous studies. In the case of  $\text{Li}_2\text{O}$ , the luminescence associated with the formation of  $\text{F}^+$  centers is observed at lower temperatures while that of  $\text{F}^0$  centers is observed at higher temperatures. Then the following reaction scheme has been given for the production mechanism of  $\text{F}^+$  and  $\text{F}^0$  centers:

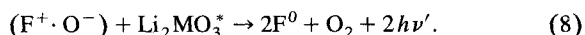
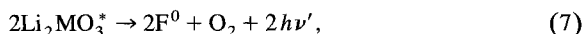
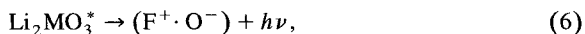


Eq. (1) represents the production of excited  $\text{Li}_2\text{O}$ ,  $\text{Li}_2\text{O}^*$ , by ion beam irradiation.  $\text{F}^+$  centers are considered to be associated with an  $\text{O}^-$  interstitial under Coulomb interaction as  $(\text{F}^+ \cdot \text{O}^-)$  and to be produced by the first-order reaction, Eq. (2). The second-order reactions, Eqs. (3) and (4), for the formation of  $\text{F}^0$  centers require some thermal activation and will take place at higher temperatures. This is the reason why the luminescence of  $\text{F}^0$  centers is

observed especially at higher temperatures. In  $\text{Li}_2\text{SiO}_3$  and  $\text{Li}_4\text{SiO}_4$ , on the other hand, the observed luminescence is connected with the formation of the peroxy species in which the second-order reactions are less important [4,5].

The present results of  $\text{Li}_2\text{TiO}_3$ ,  $\text{Li}_2\text{ZrO}_3$  and  $\text{Li}_2\text{SnO}_3$  are considered to be rather similar to those of  $\text{Li}_2\text{O}$  because of possible participation of the second-order reactions. As shown in Figs. 4–6, the temperature dependences of the luminescence intensity under  $\text{H}^+$  beam irradiation are different from those under  $\text{He}^+$  beam irradiation. Since the specific ionization is much different between both projectile ions, the reaction species concentration in each ion track will be different, and then the second-order reactions will be affected. The observed differences in Figs. 4–6 are thus suggesting the participation of such second-order reactions in the production mechanism of irradiation defects in  $\text{Li}_2\text{TiO}_3$ ,  $\text{Li}_2\text{ZrO}_3$  and  $\text{Li}_2\text{SnO}_3$ .

By the analogy of the reaction scheme for  $\text{Li}_2\text{O}$ , a production mechanism of irradiation defects in  $\text{Li}_2\text{TiO}_3$ ,  $\text{Li}_2\text{ZrO}_3$  and  $\text{Li}_2\text{SnO}_3$  is temporarily given as



Following this reaction mechanism, two types of luminescence bands are considered; one is the luminescence associated with the formation of  $\text{F}^+$  centers and the other is of  $\text{F}^0$  centers. The observed luminescence bands are thus classified into the two types. It is remembered here that the

Table 2  
Properties of ceramic breeder materials

Ceramics	Density (g cm <sup>-3</sup> )	Li density (g cm <sup>-3</sup> )	Melting point (°C)
Li <sub>2</sub> O	2.023	0.94	1423
Li <sub>2</sub> SiO <sub>3</sub>	2.52	0.36	1200
Li <sub>2</sub> TiO <sub>3</sub> (β)	3.43	0.43	1535
Li <sub>2</sub> ZrO <sub>3</sub>	4.15	0.38	1615
Li <sub>2</sub> SnO <sub>3</sub>	4.99	0.38	< 1000

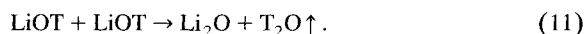
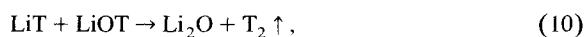
luminescence bands of shorter wave length (shorter than 340 nm) are observed more clearly at high temperatures under He<sup>+</sup> irradiation. By considering the possible participation of the secondary reactions, these bands may be attributed to F<sup>0</sup> centers. On the other hand, the luminescence bands of longer wave length (longer than 380 nm) are observed irrespective of temperature under both H<sup>+</sup> and He<sup>+</sup> irradiation and may be of F<sup>+</sup> centers.

For some details, it is interesting to compare the temperature dependences of the luminescence intensity of Li<sub>2</sub>TiO<sub>3</sub>, Li<sub>2</sub>ZrO<sub>3</sub> and Li<sub>2</sub>SnO<sub>3</sub> under H<sup>+</sup> beam irradiation. In these materials, the luminescence intensity decreases rather monotonically with increasing temperature under H<sup>+</sup> irradiation. As shown in Figs. 4–6, however, the intensity is found to decrease more rapidly in Li<sub>2</sub>SnO<sub>3</sub> than in the other two. One of the reasons may be due to different rates of the back reaction of Eq. (5) or different rates of non-radiative transition of Li<sub>2</sub>MO<sub>3</sub><sup>\*</sup>. It seems that the rate is more sensitive to temperature in Li<sub>2</sub>SnO<sub>3</sub> whose melting point is the lowest as shown in Table 2.

#### 4.3. Possible effects on tritium recovery and material stability

The production behavior of irradiation defects in Li<sub>2</sub>TiO<sub>3</sub>, Li<sub>2</sub>ZrO<sub>3</sub> and Li<sub>2</sub>SnO<sub>3</sub> is similar to those in Li<sub>2</sub>O and the irradiation defects have been observed to be formed up to blanket operating temperatures. The effects of irradiation defects on tritium recovery and material stability will thus be considered in these materials.

For the assessment of tritium release behavior of Li<sub>2</sub>O under irradiation, a model reaction scheme has been presented by taking into account the interactions of irradiation defects with tritium [9]. Tritium is produced in Li<sub>2</sub>O grains by nuclear reactions and stabilized in the chemical states of T<sup>+</sup>(LiOT) or T<sup>-</sup>(LiT). The tritium species interacts with the defect products of F<sup>0</sup> centers and O<sub>2</sub> molecules and diffuses to the grain surface, where the following surface reactions take place:



Then tritium is released in the form of T<sub>2</sub> or T<sub>2</sub>O to the sweep gas. By taking this reaction scheme, some predictions have been made and the observations in the BEATRIX-II experiment have successfully been interpreted [9].

It is important that irradiation defects participate in the reaction mechanisms at such high temperatures, because material stability will be affected as well as tritium release kinetics. In the case of H<sub>2</sub>-containing sweep gas, F<sup>0</sup> and O<sub>2</sub> are considered to react with H<sub>2</sub> at the grain surface as



Due to Eq. (13), the moisture concentration of H<sub>2</sub>O will increase with increasing H<sub>2</sub> concentration in the sweep gas, as observed in the BEATRIX-II, and then the material degradation will be accelerated in the presence of H<sub>2</sub>. Further studies are suggested accordingly.

## 5. Conclusions

(1) Multiple luminescence bands have been observed in the in situ luminescence measurement of Li<sub>2</sub>TiO<sub>3</sub>, Li<sub>2</sub>ZrO<sub>3</sub> and Li<sub>2</sub>SnO<sub>3</sub> under H<sup>+</sup> and He<sup>+</sup> ion beam irradiation. Although various types of defect species are considered to be formed in these materials, the distorted network and the different distribution of the lithium and the tetravalent cations in the network will be a possible reason for the different luminescence bands of similar origins.

(2) An interesting temperature dependence of the luminescence intensity has been observed; the luminescence intensity under He<sup>+</sup> ion irradiation rises at the temperatures around 700 K while it decreases rather monotonically with increasing temperature under H<sup>+</sup> irradiation. In the temperature range where the luminescence intensity rises under He<sup>+</sup> irradiation, the luminescence bands of shorter wave length (shorter than 340 nm) are observed more clearly in the spectra. From these findings, it has been suggested that the production mechanism of irradiation defects in these materials is similar to that in Li<sub>2</sub>O.

(3) Irradiation defects are formed even at the blanket operating temperatures, and the effects on tritium recovery and material stability have been pointed out by considering the participation of F<sup>0</sup> centers and O<sub>2</sub> molecules in the reaction mechanisms. These species may react with hydrogen in the sweep gas and accelerate the degradation of the materials.

## Acknowledgements

The authors wish to thank Mr K. Yoshida, Kyoto University, for his kind encouragements.

## References

- [1] Y. Asaoka, H. Moriyama, K. Iwasaki, K. Moritani, Y. Ito, J. Nucl. Mater. 183 (1991) 174.
- [2] Y. Asaoka, H. Moriyama, Y. Ito, Fusion Technol. 21 (1992) 1944.
- [3] Y. Asaoka, H. Moriyama, K. Iwasaki, K. Moritani, Y. Ito, J. Nucl. Mater. 191–194 (1992) 268.
- [4] H. Moriyama, T. Nagae, K. Moritani, Y. Ito, in: Fusion Technology 1992, eds. C. Ferro, M. Gasparotto and H. Knoepfel (North-Holland, Amsterdam, 1993) p. 1434.
- [5] H. Moriyama, T. Nagae, K. Moritani, Y. Ito, Nucl. Instrum. Methods B91 (1994) 317.
- [6] V. Grishmanov, S. Tanaka, Proc. of 4th Int. Workshop on Ceramic Breeder Blanket Interactions, Kyoto, Oct. 9–11, 1995, p. 153.
- [7] J.L. Hodeau, M. Marezio, A. Santoro, R.S. Roth, J. Solid State Chem. 45 (1982) 170.
- [8] J.F. Dorrian, R.E. Newnham, Mater. Res. Bull. 4 (1969) 179.
- [9] H. Moriyama, T. Kurasawa, J. Nucl. Mater. 212–215 (1994) 932.